

# Modified discontinuous deformation analysis for rock failure: Crack propagation

Yunjuan Chen<sup>\*1</sup>, Xin Zhang<sup>1</sup>, Weishen Zhu<sup>2</sup> and Wen Wang<sup>3</sup>

<sup>1</sup>School of Civil Engineering, Shandong Jianzhu University, Ji'nan 250101, Shandong, China

<sup>2</sup>Geotechnical and Structural Engineering Research Center, Shandong University, Ji'nan 250061, Shandong, China

<sup>3</sup>Shandong Urban Construction Vocational College, Ji'nan 250103, Shandong, China

(Received August 9, 2016, Revised July 31, 2017, Accepted August 7, 2017)

**Abstract.** Deformation of rock masses is not only related to rock itself, but also related to discontinuities, the latter maybe greater. Study on crack propagation at discontinuities is important to reveal the damage law of rock masses. DDARF is a discontinuous deformation analysis method for rock failure and some modified algorithms are proposed in this study. Firstly, coupled modeling methods of AutoCAD-DDARF and ANSYS-DDARF are introduced, which could improve the modeling efficiency of DDARF compared to its original program. Secondly, a convergence criterion for automatically judging the computation equilibrium is established, it could overcome subjective drawbacks of ending one calculation by time steps. Lastly but not the least, relationship between the super relaxation factor and the calculation convergence is analyzed, and reasonable value range of the super relaxation factor is obtained. Based on these above modified programs, influences on crack propagation of joint angle, joint parameters and geo-stresses' side pressure are studied.

**Keywords:** crack propagation; discontinuous deformation analysis method for rock failure (DDARF); coupled modeling methods; convergence criterion

## 1. Introduction

Study on crack propagation is of great importance to analyze the stability of rock masses (Haeri *et al.* 2013, 2014, 2015, Mohammadi *et al.* 2015, Liu *et al.* 2016, Wang *et al.* 2016), and there is no doubt that numerical simulation is an effective method for it (Haeri *et al.* 2013, 2014, 2015, Behnia *et al.* 2014). By now, various kinds of numerical methods for simulating crack propagation have appeared (Zhou *et al.* 2015, Yang *et al.* 2012, Zhou *et al.* 2014), including meshless methods (Asphaug 1995, Rabczuk and Zi 2007), DMM (Scavia 1999, Vasarhelyi and Bobet 2000), EFG (Belytschko and Lu 1994), SPH (Nirouman *et al.* 2016, Libersky *et al.* 1993), DEM (Vesga *et al.* 2008), PFC (Yoon 2007, Zhang and Wong 2012, Lee and Jeon 2011). They are adopted to simulate the growth of crack and have gotten certain useful results, while, some of them have their own shortcomings, for example, the EFG method must add a lot of nodes along crack growth paths and the SPH method has difficulty in accurately simulating the coalescence process of cracks, and so on.

DDA is originally proposed by Shi G.H. (1998, 1999), which combines the advantages of FEM

and DEM method. It can not only obey the rigorous mathematical theory but also simulate the large deformation or large displacement, and widely used in analyzing rock masses' stabilities. Based on the framework of DDA, a new

discontinuous deformation analysis method for rock failure (DDARF) is put forward by Jiao and Zhang (2010, 2007), in order to describe the whole failure process of rock mass, especially for the intermittent jointed rock mass. In this method, the block boundary is defined as artificial joint, when the artificial joint reaches its ultimate strength, it will become to be real joint and its mechanical parameters will decrease accordingly.

It is no more than 10 years since DDARF appeared, although it can well describe the crack propagation process, yet, it still has some algorithms needing to be improved. This paper is mainly focused on the pre-treatment modeling programs and convergence programs, and thus to improve DDARF's simulation efficiency and precision. With these modified algorithms, influences of joint angle, joint parameters and side pressure coefficient on crack propagation will be analyzed.

The paper is organized as follows. In Sect. 2, the fracturing mechanism of DDARF is demonstrated and some of its shortcomings are briefly outlined. Modified algorithms with respect to the pre-treatment modeling (including AutoCAD-DDARF coupled modeling program and ANSYS-DDARF coupled modeling program) and the calculation convergence criterion are proposed in Sect. 3. Influences on crack propagation of joint angle, joint parameters and side pressure coefficient are analyzed in Sect. 4. And conclusions are summarized in Sect. 5.

## 2. Background

DDA has three main features: (1) displacements' first-

\*Corresponding author, Ph.D.  
E-mail: [skdcyj@126.com](mailto:skdcyj@126.com)

order approximation, (2) the principle of minimum potential energy, and (3) kinematic conditions of no embedding and no stretching. DDARF is a modified software based on DDA (Jiao *et al.* 2014, 2015), besides all the characteristics of DDA and meanwhile it also has its own traits: (1) study domain is subdivided into multiple triangular blocks, (2) blocks' mechanical parameters are of Weibull distribution; (3) blocks' boundaries offer paths for crack propagation.

### 2.1 Fracturing mechanism of DDARF

When the study domain is divided into triangular blocks, boundary will be generated, which provides the possible path for crack propagation. The block boundary is defined as artificial joint, where adding a set of springs, one is normal and the other is tangential. And normal spring should obey the maximum tensile stress criterion (Eq. (1)), tangential spring should obey the Mohr-Coulomb criterion (Eq. (2)).

$$f_n = -T_0 l \tag{1}$$

$$f_\tau = cl + f_n \tan \varphi \tag{2}$$

where  $f_n$  and  $f_\tau$  are contacting force of the normal spring and the tangential spring, respectively.  $T_0$  is the axial tensile strength of rock mass,  $C$  is the cohesion of rock mass,  $\varphi$  is the friction angle of rock mass, and  $l$  is the contacting length.

The artificial joint is considered to have characteristics of viscous cracks (Fig. 1), and thus the constitutive model of normal spring in DDARF can be modified as

$$\begin{cases} f_n = k_1 d, d < d_0 \\ f_n = k_1 d_0 \frac{d_c - d}{d_c - d_0}, d_0 < d < d_c \end{cases} \tag{3}$$

where  $k_1$  is the stiffness of contacting springs,  $d$  is block's opening displacement,  $d_0$  is the opening displacement when the normal cohesion reaches its maximum tensile strength, and  $d_c$  is the opening displacement when the normal cohesion becomes zero.

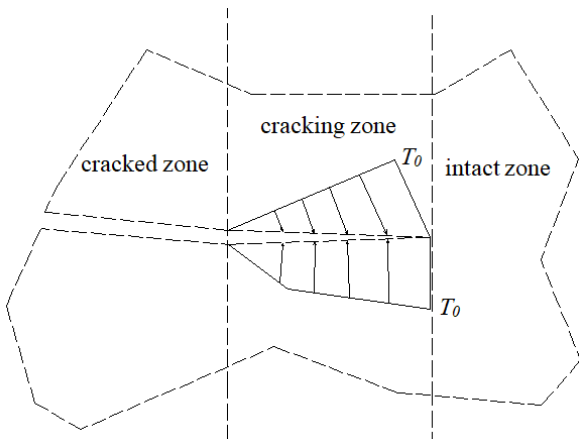


Fig. 1 Fracturing process of sticky crack model

When  $d \leq d_0$ , the contacting sub-matrices can be expressed as

$$\begin{aligned} k_1 \mathbf{E}_i^T \mathbf{E}_i &\rightarrow \mathbf{K}_{ii}, & k_1 \mathbf{G}_i^T \mathbf{G}_i &\rightarrow \mathbf{K}_{jj} \\ k_1 \mathbf{E}_i^T \mathbf{G}_j &\rightarrow \mathbf{K}_{ij}, & k_1 \mathbf{G}_j^T \mathbf{E}_i &\rightarrow \mathbf{K}_{ji} \\ -\frac{s_0}{l} k_1 \mathbf{E}_i &\rightarrow \mathbf{F}_i, & -\frac{s_0}{l} k_1 \mathbf{G}_j &\rightarrow \mathbf{F}_j \end{aligned} \tag{4}$$

and when  $d > d_0$ , the contacting sub-matrices can be expressed as

$$\begin{aligned} -k_2 \mathbf{E}_i^T \mathbf{E}_i &\rightarrow \mathbf{K}_{ii}, & -k_2 \mathbf{G}_i^T \mathbf{G}_j &\rightarrow \mathbf{K}_{jj} \\ -k_2 \mathbf{E}_i^T \mathbf{G}_j &\rightarrow \mathbf{K}_{ij}, & -k_2 \mathbf{G}_j^T \mathbf{E}_i &\rightarrow \mathbf{K}_{ji} \\ \left(\frac{s_0}{l} - d_c\right) k_2 \mathbf{E}_i &\rightarrow \mathbf{F}_i, & \left(\frac{s_0}{l} - d_c\right) k_2 \mathbf{G}_j &\rightarrow \mathbf{F}_j \end{aligned} \tag{5}$$

where

$$k_2 = \frac{(T_0 l)^2}{2G_{1c} l - \frac{(T_0 l)^2}{k_1}} \tag{6}$$

If the block's opening displacement is too large and it reaches  $d_c$ , the bonding force of springs will fail, then, the artificial joint is converted into real joint (Jiao *et al.* 2010).

### 2.2 Shortcomings of DDARF's original programs

#### 2.2.1 Pre-treatment modeling program

In DDARF, calculation model is established by the DL program and the DC program. The function of DL program is to generate random joints network and the function of DC program is to generate triangular blocks, as well as store all the geometrical information. In the modeling process, caverns must have regular geometrical shapes, such as circle, rectangle, horseshoe, etc. The original program can hardly simulate caverns with irregular corners or random joints, and simulation cannot be guaranteed to succeed every time. In a word, only simple models can be generated by the original pre-treatment modeling program.

#### 2.2.2 Calculation convergence algorithm

In the original numerical simulation, users stop one calculation usually by inputting time steps, it has big subjectivity and the accuracy mainly depends on numerical experience of the operators. From this perspective, it is necessary to establish a reasonable convergence criterion which can judge system's equilibrium automatically. At the same time, influences of the super relaxation factor on calculation convergence have never been analyzed, while, as a matter of fact, the super relaxation factor may determine the convergence speed and even whether the program converges or not.

These above two shortcomings of DDARF have reduced its calculation precision and efficiency, so it is urgent to find new algorithms to overcome the disadvantages and thus promote DDARF's simulation on crack propagation.

## 3. Modified algorithms

### 3.1 Coupled modeling program

Calculation model can be established in another software and then imported into DDARF, it is a good way to improve the modeling efficiency. Herein, two modeling software is introduced and their modeling methods are presented in details.

### 3.1.1 AutoCAD-DDARF modeling methods

As a drawing tool, AutoCAD has great drawing function, easily to use and develop. Users can profile an .ARX file in the VC++ environment, it shares the common codes with original AutoCAD. In the .ARX file, we could define our own algorithms, such as methods to generate various kinds of lines, points or joints, etc. Among them, random joints would be generated by the Monte-Carlo method, with four geometrical distributions defined, including Uniform Distribution, Fixed Distribution, Exponential Distribution and Normal Distribution.

One advantage of this method is that we can adjust model's unbefitting lines or points easily, such as numbers or locations of the random joints. In DDARF, when the total lines are more than 200, the computation would hardly continue, then joints' density far away from cavern (Fig. 2(a)) needs to be reduced. In the same way, if one cavern has some strange corners and then cannot be established with the original program, it also can be drawn in AutoCAD (Fig. 2(b)). All figures drawn in AutoCAD can be imported into DDARF by the .ARX file. It should be noted that, this method can only generate model's figure, and its grids still need to be divided in DDARF itself.

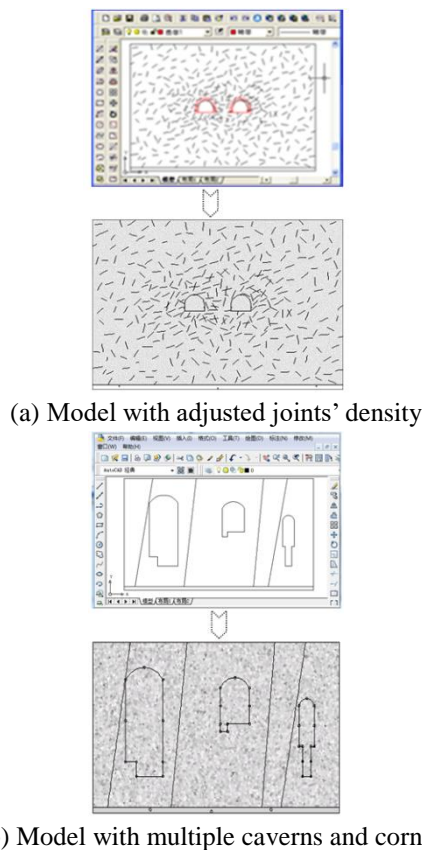


Fig. 2 Calculation model established from AutoCAD to DDARF

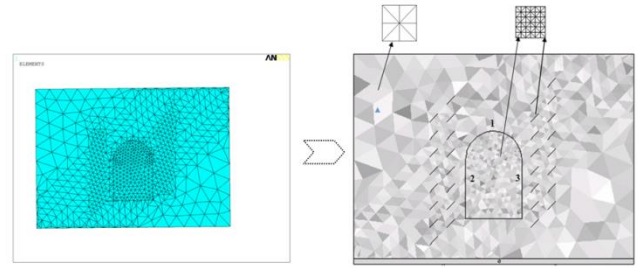


Fig. 3 Calculation model established from ANSYS to DDARF

### 3.1.2 ANSYS-DDARF modeling methods

As a general finite element analysis method, ANSYS has very strong modeling function with higher visualization. In ANSYS, model with complex shapes can be divided into multiple sub-parts and every sub-part may have different grid density according to needs. For example, areas with large data gradient would have dense grids, and areas with small data gradient may have relatively sparse grids. Relationship between the total grid scales and calculation efficiency can be well optimized by this method. Based on advantages of ANSYS modeling program, DDARF's calculation model can be gotten indirectly, as shown in Fig. 3 (Wang 2014), and this modeling method is as follows in detail.

(1) Calculation model is established and divided into multiple grid elements in ANSYS.

(2) Information of model's nodes and elements can be read in ANSYS, and saved as separate files. The nodes and elements have their own number, and the number must be counterclockwise.

(3) APDL file is compiled and then the coupled program of ANSYS-DDARF is built, all the information of model's nodes and elements can be called, and at the same time model's boundary lines and other geometrical information are defined.

It should be noted that, what gotten in this modeling method is only nodes' displacement information, rather than element centers' displacement variables, as a result, before calling the model from ANSYS, all the sub-matrixes and their contributions to the overall equilibrium equations should be firstly re-derived, and then compiled into the DF file (DDARF' computation file).

In a word, AutoCAD-DDARF modeling method and ANSYS-DDARF modeling method can improve the modeling efficiency with their own characteristics, while, they still have their common points, what they can adjust is only the geometrical figures, and they both cannot change DDARF's algorithms, that is to say, based on these two modeling methods, modified DDARF is still a discontinuous deformation analysis for rock failure.

## 3.2 Calculation convergence and affection by the super relaxation factor

### 3.2.1 Theory on calculation convergence

The original program of DDARF cannot judge whether a system balances or not automatically, it usually terminates the computation by inputting time steps, and this has big

subjectivity. Calculation accuracy depends largely on the experience of operators. Suitable time steps can guarantee that the solving does not float near the true solution. If time steps are too little, the system will fail in advance, while, if time steps are too much, it will reduce the simulation efficiency. Appropriate convergence criterion can ensure the calculation accuracy and efficiency simultaneously. Many parameters can be used as the criterion parameters, such as displacement or the maximal unbalanced force, here, in order to operate simply and strongly, a displacement convergence criterion, reliable and widely used in other numerical methods, is adopted in DDARF.

When a block system tends to be stable, the displacement difference of adjacent two time steps will also tend to be zero. Assuming that a block system includes  $m$  blocks, the displacement of block  $i$  at time-step  $n$  is  $D_i^n$ , its displacement difference is  $\Delta D_i^n$ , and then the displacement convergence criterion can be presented as

$$\frac{\Delta D_i^n}{D_i^n} < \varepsilon \tag{7}$$

where  $\varepsilon$  is preferred to be  $10^{-5}$ - $10^{-2}$ , according to needs. Of course,  $D_i^n$  and  $\Delta D_i^n$  can be replaced by other variables, such as stresses, which mainly depend on research purpose.

DDARF's computation uses the Successive Over Relaxation method (SOR), it requires lower computer storage and thus can reduce the computation load greatly.

$$x^{k+1} = x^k + \omega r^k \tag{8}$$

where,  $k=0,1,2\Lambda ,n$ , which is the iteration number,  $\omega$  is the super relaxation factor and in the SOR method,  $\omega > 1$ . For the same equation, the super relaxation factor has prodigious influence on the computation stability, if the super relaxation factor is improper, it will affect the calculation convergence and even lead to non-convergence.

### 3.2.2 Engineering application

An underground cavern is to be excavated and there are two groups of random joints. Joints' direction, length and spacing respectively obeys Normal Distribution, Uniform Distribution and Exponential Distribution, their geometrical information is shown in Table 1. Size of calculation model is 50 m×35 m (width×height) and size of cavern is 10 m×15 m (width×height). Take those modified algorithms into the discontinuous deformation analysis, including the AutoCAD-DDARF modeling method and the displacement convergence criterion. At the same time, influence on convergence of the super relaxation factor is considered and  $\varepsilon$  is taken to be  $10^{-3}$ . Calculation model established by AutoCAD-DDARF is shown in Fig. 4 and the numerical parameters are presented in Table 2.

Table 1 Geometrical parameters of random joints

random joints	joint space/m	joint length/m		joint direction/(°)	
		mean value	square error	mean value	square error
1	4	8	3	60	5
2	4	8	2	120	8

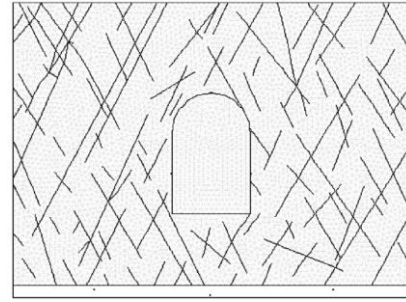
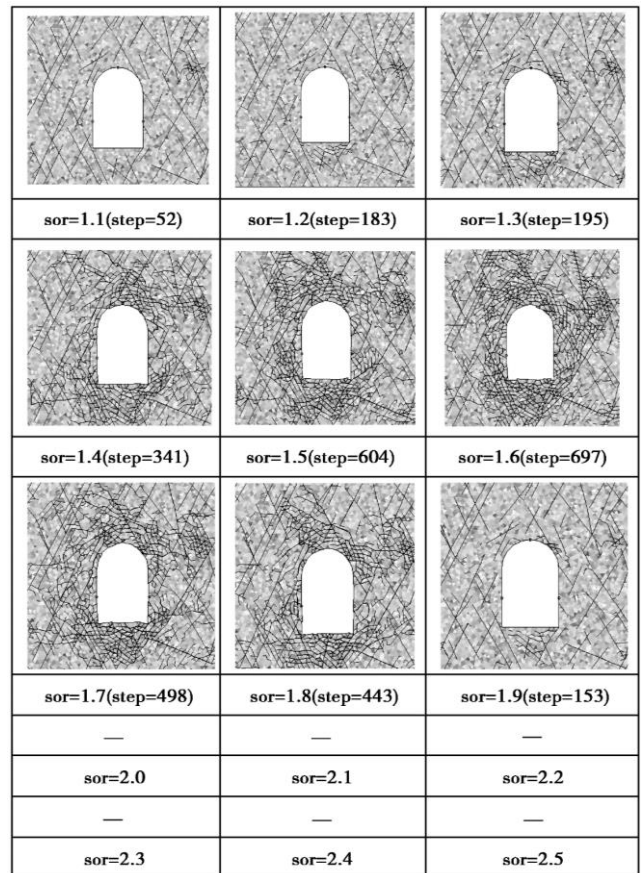


Fig. 4 Underground cavern model established from AutoCAD to DDARF

Table 2 Numerical parameters of calculation model

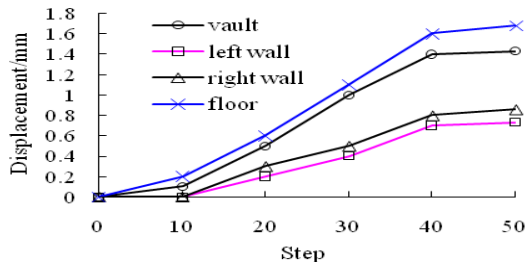
classes	density /( $g/cm^3$ )	elastic modulus/GPa	poisson's ratio	friction angle/(°)	cohesion/MPa	tensile strength/MPa
rock mass	2.61	20	0.25	30	5	1.8
virtual joint	-	-	-	30	5	1.8
real joint	-	-	-	30	0	0



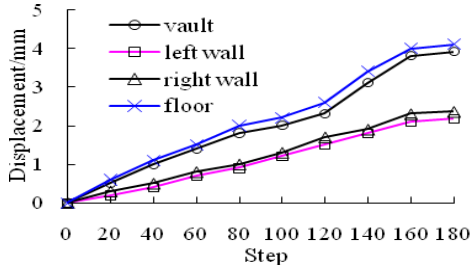
Note: “—” represents that the calculation can't compute and “sor” represents the super relaxation factor.

Fig. 5 Surrounding rock masses' crack propagation versus convergence steps

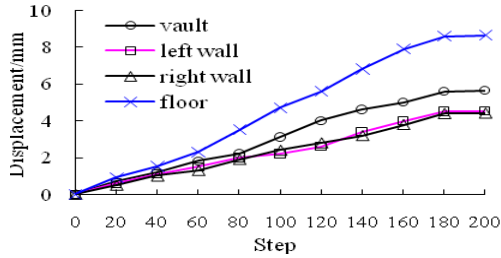
When the computation is converged, the total time steps and surrounding rock masses' crack propagation are different as the super relaxation factor changes, as shown in Fig. 5.



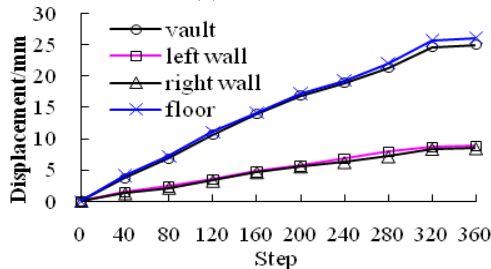
(a) sor=1.1



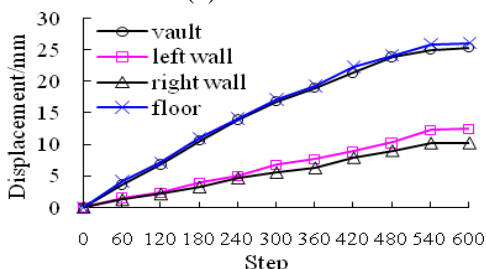
(b) sor=1.2



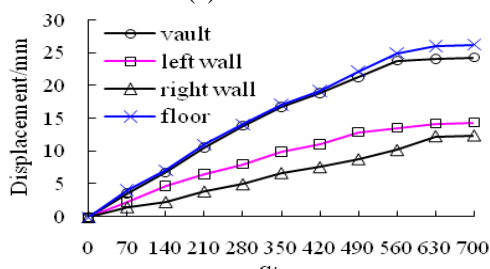
(c) sor=1.3



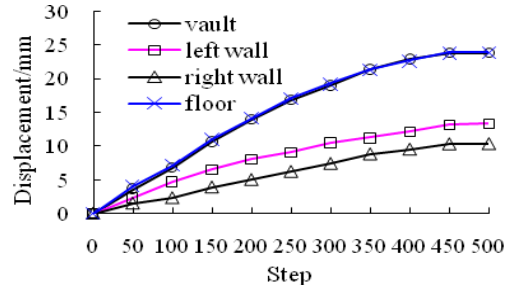
(d) sor=1.4



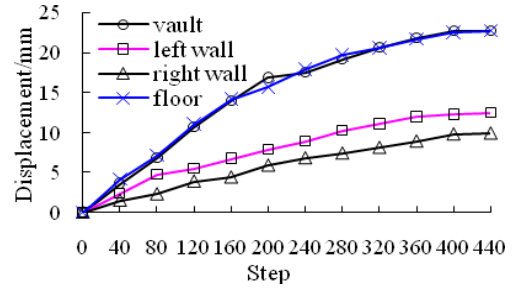
(e) sor=1.5



(f) sor=1.6



(g) sor=1.7



(h) sor=1.8

Fig. 6 Continued

As it can be observed, cavern's vault and floor can be affected greatly by excavation and the propagated cracks are mainly concentrated in these two parts. When the super relaxation factor values in the range of 1.4-1.8, computation results are relatively stable and the crack propagation has little changes, which are in line with the numerical experience. When the super relaxation factor is less than or equal to 1.3, numerical simulation becomes coarse and this calculation will have lower accuracy. While, when the super relaxation factor is greater than or equal to 2.0, the calculation cannot converge.

Midpoints of cavern's vault, floor, left and right walls are taken to be key points, and when calculation converges, the key points' displacements are shown in Fig. 6.

Fig. 6 indicates that, there are little displacement differences when the super relaxation factor changes from 1.4 to 1.8, the maximum displacement occurs at the vault and floor of this cavern, reaches 25mm or so. When the super relaxation factor values in the range of 1.4-1.8, computation results are relatively stable, and in good agreement with that of crack propagation. In this analysis, the reasonable value range of super relaxation factor is considered to be 1.4-1.8.

In addition, crack propagation of cavern's vault and floor is obvious at this stress state, and their displacements are also relatively large, hence, some appropriate support measures should be taken to ensure the stability of surrounding rock masses.

#### 4. Numerical simulation on crack propagation

On the basis of those above studies, influences of joint angle, joint parameters and geo-stresses' side pressure on rock masses' crack propagation are analyzed. In the following numerical studies, the super relaxation factor is taken to be 1.5.

Fig. 6 Displacements of cavern's key points with different super relaxation factors

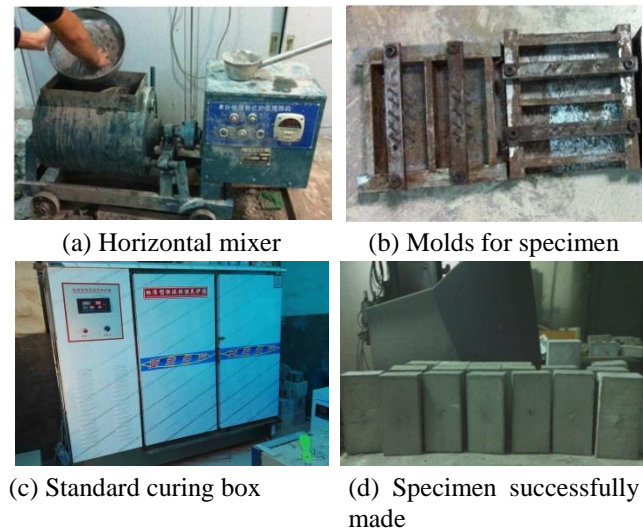


Fig. 7 Molds and specimen made

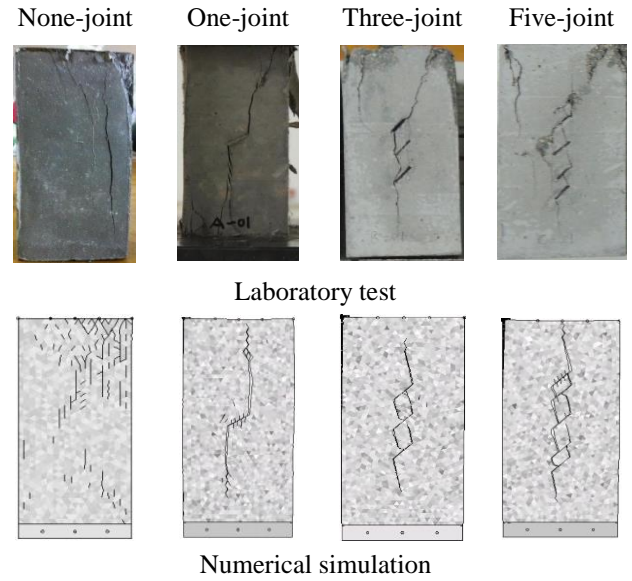


Fig. 8 GAW-2000 rigid testing machine

4.1 Influence on crack propagation of joint angle

To verify the modified algorithms of DDARF, a set of laboratory tests for crack propagation with different joint angles are firstly done. In the laboratory test, river sand, portland cement, water-reducing agent and water are chosen as the specimen materials according to multiple ratio-analyses, their quality ratio is 0.8:1:0.03:0.3. Joint is made of polyvinyl chloride (PVC), its length is 15 mm and the thickness is 0.5 mm. Size of the specimen is 70 m×45 m×140 m (length×width×height), it would be maintained for 1-2 weeks or so in a standard curing box, in order to improve the strength of specimen. The molds and specimen made are shown in Fig. 7.

Restricted by the molds, joint angle can only make to be 30°, 45° and 60°. Take none-joint specimen, one-joint specimen, three-joint specimen and five-joint specimen for example, the laboratory test and numerical simulation are both done and their differences on crack propagation are compared. Laboratory test is done with the GAW-2000 testing machine (shown in Fig. 8), controlled by displacement with the rate of 0.1 mm/min, its whole process of crack propagation is recorded by a DV camera. And numerical simulation is based on the mechanical results gotten by this laboratory test, they have the same physical and mechanical conditions. In the meantime, AutoCAD-DDARF modeling method and displacement convergence criterion are used in the numerical simulation. Results of the laboratory test and numerical simulation are shown in Fig. 9.



(a) Crack propagation of specimen

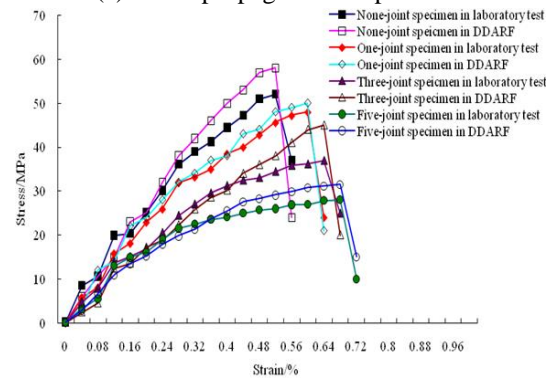
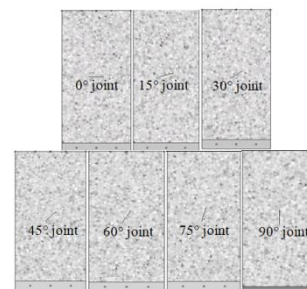
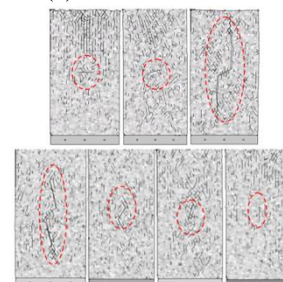


Fig. 9 Results of the laboratory tests and numerical simulations



(a) Numerical model



(b) Crack propagation

Fig. 10 Crack propagation of specimen with different joint angles

Fig. 9 shows the high consistency of laboratory test and numerical simulation, their cracks possess the similar propagating shapes and scales, meanwhile, their stress-strain curves all have the obvious elastic-brittle characteristics. This similarity proves the feasibility and rationality of those modified algorithms of DDARF. On the basis of these modified algorithms, the following will give studies on crack propagation with different joint angles, shown in Fig. 10.

Fig. 10 shows that, when the joint angle is equal to 0°, 15°, 75°, or 90°, specimen's secondary cracks arise and propagate with the increase of axial load. While influences of original joints can be negligible and there are no wing-cracks. When the joint angle is equal to 30°, 45° or 60° especially 30° and 45°, some secondary cracks also exist but influences of original joints become large, and meanwhile, there are obvious wing-cracks, their propagating directions are parallel to that of the maximum principal stress. So, if there are multiple joints with angle of 30° or 45° in the surrounding rock masses, the split-fracture would appear and should be paid attention. Mohr-Coulomb constitutive model may be no longer reasonable, and the split constitutive model or the plate-crack structure theory will be more appropriate to analyze rock masses' stabilities. In a word, when the joint angle is equal to 0°, 15°, 75°, or 90°, secondary cracks should be prevented and when the joint angle is equal to 30°, 45° or 60° especially 30° and 45°, original joints' wing-cracks should be paid more attention.

4.2 Influence on crack propagation of joint parameters

In order to analyze joint parameters' influence on crack propagation, a calculation model with two parallel joints is established by AutoCAD-DDARF modeling method. The total grid number is 1200, its size is 70 m×140 m (width×height), two joints' lengths are both 20 mm and their angles are both 30°, these two joints are alignment and their vertical spacing is 25 mm, which is shown in Fig. 11. The numerical model is compressed by the axial force and calculate with 250 steps, its physical and mechanical parameters are presented in Table 3.

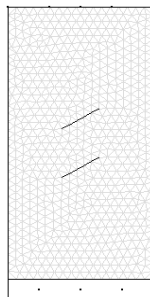


Fig. 11 Calculation model with two parallel joints

Table 3 Mechanical parameters of numerical simulation

classes	density /( $g/cm^3$ )	elastic modulus/GPa	poisson's ratio	friction angle/(°)	cohesion/MPa	tensile strength/MPa
rock mass	2.61	15	0.15	56	2.5	5.8
virtual joint	-	-	-	35	2.0	3.5

Table 3 Continued

classes	density /( $g/cm^3$ )	elastic modulus/GPa	poisson's ratio	friction angle/(°)	cohesion/MPa	tensile strength/MPa
real joint	-	-	-	30	0	0

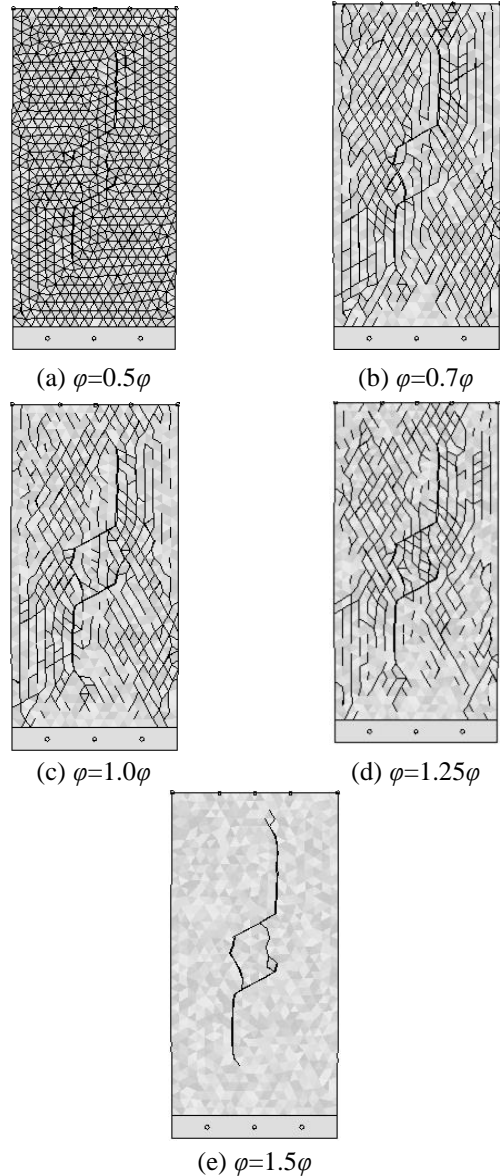


Fig. 12 Sensitivity analysis of friction angle on crack propagation

Meanwhile, joints' parameters are multiplied by 0.5, 0.75, 1.0, 1.25 and 1.75 times of that in Table 3 and the sensitive influences of friction angle  $\phi$ , cohesion  $c$  and tensile strength  $t$  on crack propagation are summarized, numerical results are shown in Figs. 12, 13 and 14, respectively.

As it can be seen from Fig. 12, as friction angle changes, scales and forms of propagating cracks change accordingly. When the friction angle is equal to 0.5 times by that in Table 3, the specimen has been completely broken, while as the friction angle increases, the specimen's damage degree is controlled obviously and when the friction angle reaches 1.5 times by that in Table 3, the specimen will keep intact

and there are no cracks. Therefore, increase of friction angle can inhibit propagation of both secondary cracks and wing-cracks effectively.

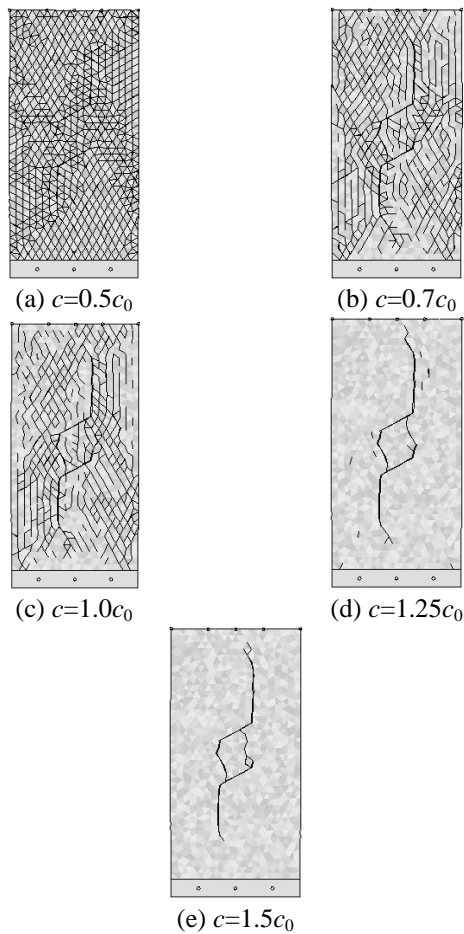


Fig. 13 Sensitivity analysis of cohesion on crack propagation

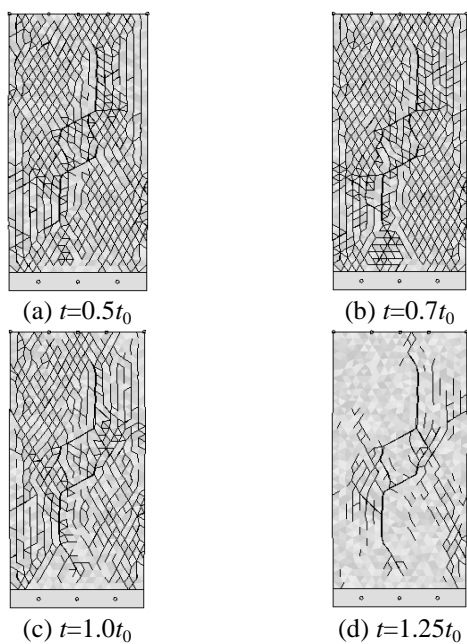


Fig. 14 Sensitivity analysis of tensile strength on crack propagation



Fig. 14 Continued

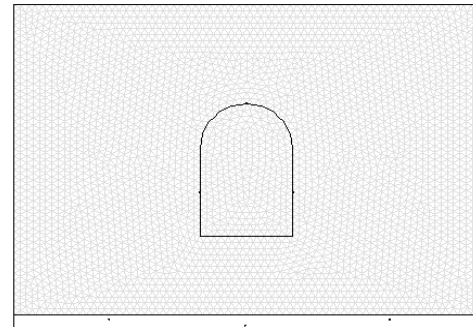


Fig. 15 Numerical model of underground cavern without joints

Table 4 Mechanical parameters of numerical model

Classes	Density /( $\text{g}/\text{cm}^3$ )	Elastic modulus/GPa	Poisson's ratio	friction angle/( $^\circ$ )	cohesion/MPa	tensile strength/MPa
Rock mass	2.65	20	0.25	45	6.5	6.8
Virtual joint	-	-	-	36	4.6	5

Fig. 13 shows that crack propagation is limited gradually along with the increase of joints' cohesion. While compared to Fig. 12, it should be noted that joints' cohesion mainly controls secondary cracks' propagation, and it has minor influence on original joints' wing-cracks, propagating direction of wing-cracks is still parallel to the axial direction.

It shows up in Fig. 14, inhibition on crack propagation of tensile strength is as the same as that of the cohesion, and similarly, increase of tensile strength can greatly control propagation of the secondary cracks, while has little influence on the wing-cracks.

Improving joints' strength can effectively control crack propagation and thus ensure the stability of rock masses. From all the changes of cracks' scales, quantities and forms, we can get it that friction angle's sensitivity on crack propagation is the biggest, followed by the cohesion, and the last one is joints' tensile strength.

#### 4.3 Influence on crack propagation of geo-stresses' side pressure

Geo-stresses' side pressure cannot be ignored and it usually has great influence on stabilities of rock masses. Here, underground cavern engineering with different joints' distributions are studied, in order to analyze the influence of geo-stresses' side pressure on surrounding rock masses'

crack propagation.

4.3.1 Underground cavern without joints

A cavern is deep in 400 m or so, its excavation size is 10 m×15 m (span×height), and the computing model's size is 50 m×35 m (length×height), there are no obvious joints in the calculation model, as shown in Fig. 15. Force focused on the calculation model is mainly gravity of rock masses, and geo-stresses' side pressure coefficient is taken to be  $K_0=0.5$ ,  $K_0=1.0$  and  $K_0=1.5$ , to analyze its influence on crack propagation. This cavern is excavated with three average steps and the mechanical parameters are presented in Table 4, the numerical converged results are shown in Fig. 16.

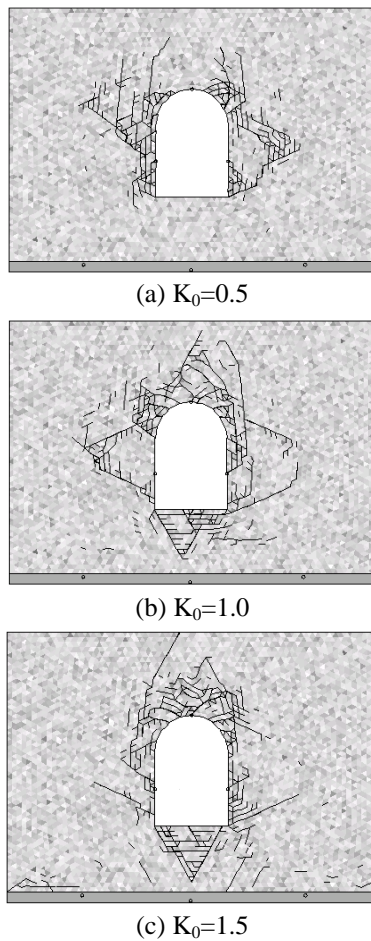
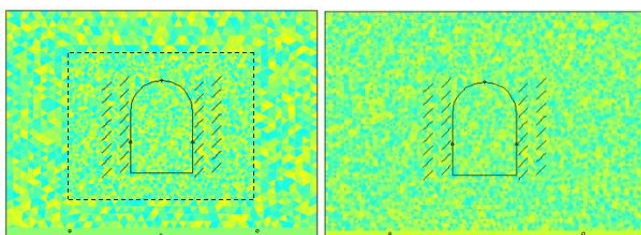


Fig. 16 Surrounding rock masses' crack propagation of cavern without joints



(a) Multi-scale grid model A (b) Uniform grid model B

Fig. 17 Calculation model of cavern excavation

Fig. 16 gives the obvious results that, when geo-stresses' side pressure coefficient is equal to 0.5, propagated cracks are almost concentrated in both sides of this cavern, there are no secondary cracks in the vault or floor. When geo-stresses' side pressure coefficient is equal to 1.0, cracks appear in all directions of surrounding rock masses, and there are no distinct difference in every direction. When geo-stresses' side pressure coefficient is equal to 1.5, propagating area is converted from the left and right sides to the vault and floor, cavern excavation's influence on the vault and floor is much bigger than that on both sides. In other words, as the increase of  $K_0$ , cracks propagate gradually from both sides to the vault and floor of this cavern.

4.3.2 Underground cavern with parallel joints

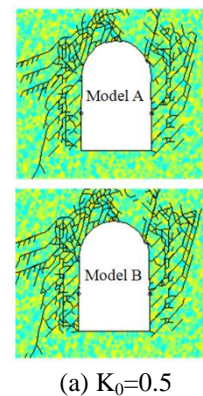
A set of parallel joints are in the calculation model, joints' lengths are all 2m and their angles are all 45°. Multi-scale grid meshing method and uniform grid meshing method are used to establish this calculation model (Zhu *et al.* 2014). In multi-scale grid model A, areas around the cavern have dense grids and their grid densities are almost two times as that of areas far away, the total grid number is 5000, shown in Fig. 17(a). In uniform grid model B, its grid density is the same as that of the dense grid areas in model A, while its total grid number is up to 8000, shown in Fig. 17(b). These two models' geometrical parameters are the same as those of calculation model in Fig. 15, and their mechanical parameters are shown in Table 5.

Cavern excavation still uses three steps and the numerical results of crack propagation with different geo-stresses' side pressure are shown in Fig. 18.

As shown in Fig. 18, for the cavern with parallel joints, influence of geo-stresses' side pressure on crack propagation is the same as that of cavern without joints. As the increase of  $K_0$ , cracks also propagate from the left and

Table 5 Mechanical parameters of parallel joints model

Classes	Density /( $g/cm^3$ )	Elastic modulus/GPa	Poisson's ratio	Friction angle/(°)	Cohesion /MPa	Tensile strength/MPa
Rock mass	2.65	20	0.25	45	6.5	6.8
Virtual joint	-	-	-	36	4.6	5
Real joint	-	-	-	30	0	0



(a)  $K_0=0.5$

Fig. 18 Crack propagation of surrounding rock mass with different geo-stresses' side pressure

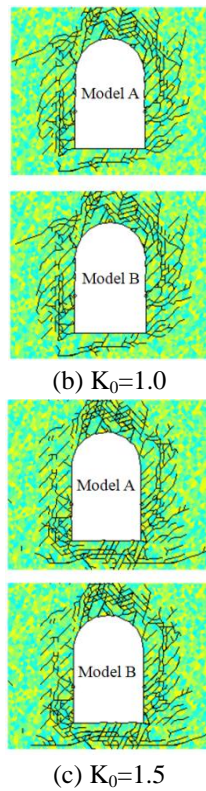


Fig. 18 Continued

right sides to the vault and floor. Even when the  $K_0$  is equal to 1.5, the scales and quantities of cracks caused by original parallel joints are smaller than those of cracks in the vault and floor. Under this condition, influence on crack propagation of geo-stresses' side pressure is bigger than that of original joints.

4.3.3 Underground cavern with random joints

Compared to calculation model with parallel joints, the only difference of this cavern is that its joints are random. Joints' geometrical parameters are taken to be the same as Table 1. The length obeys Uniform Distribution, angle obeys Normal Distribution and spacing obeys Exponential Distribution. Calculation model is shown in Fig. 19 and numerical results are shown in Fig. 20.

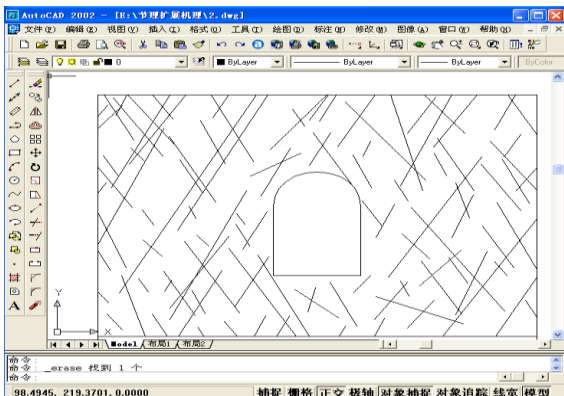
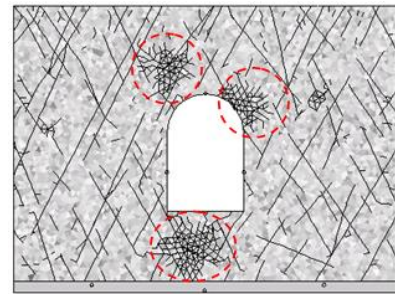
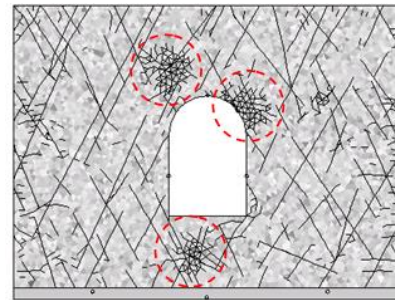


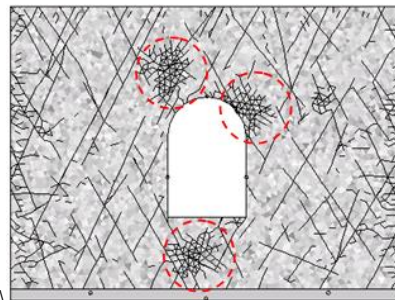
Fig. 19 Random joints model established in AutoCAD



(a)  $K_0=0.5$



(b)  $K_0=1.0$



(c)  $K_0=1.5$

Fig. 20 Crack propagation of surrounding rock mass with different geo-stresses' side pressure

Fig. 20 shows that, cracks' propagating law cannot be changed by geo-stresses' side pressure. In the surrounding rock masses of this cavern, they all have three parts (the dashed circle lines shown in Fig. 20) with relatively dense cracks. Cavern excavation mainly leads to crack propagation in these three parts, where release energy and keep the balance of rock masses. Meanwhile, the influence of cavern excavation in other areas can be ignored. So, if there are several random joints in surrounding rock masses, crack propagation will be largely affected by parameters of random joints, rather than geo-stresses' side pressure.

In a word, if there are no joints or joints can be ignored, influence of geo-stresses' side pressure on crack propagation will be great. As  $K_0$  increases, cracks will propagate from cavern's both sides to the vault and floor. While if there are obvious joints, crack propagation will be affected by joints' distributions and parameters more, compared to geo-stresses' side pressure.

5. Conclusions

Some modified programs of DDARF to simulate crack propagation are presented in this paper, new modeling

methods such as AutoCAD-DDARF and ANSYS-DDARF coupled algorithms are formed, and its own calculation convergence criterion is also established. Based on these modified algorithms of DDARF, influences of joint angle, joint parameters and geo-stresses' side pressure on crack propagation are analyzed, major conclusions include:

- Wing-cracks usually propagate with joint angle of 30°, 45° or 60°, and parallel to the maximum stresses' direction. Rocks are relatively safer with joint angle of 0°, 15°, 75°, or 90° and the propagating cracks are mainly secondary cracks, rather than wing-cracks.

- Joints' friction angle has the greatest sensitivity on crack propagation of rock masses, followed by the cohesion, and the last one is joints' tensile strength.

- If there are no joints or joints are not obvious, cracks will propagate from cavern's both sides to the vault and floor as geo-stresses' side pressure increases. While, if the joints cannot be ignored, crack propagation will be largely affected by joints' distributions and parameters.

## Acknowledgments

This work was supported by the National Natural Science Foundation of China (51609130, 51678350 & 51509145), the China Postdoctoral Science Foundation Funded Project (2015M582092 & 2016M592213), the Innovation Team Program of Education Ministry of China (IRT13075) and Shandong Provincial Natural Science Foundation (ZR2016EEQ10 & ZR2015EQ005). Great appreciation goes to the editorial board and the reviewers of this paper.

## References

- Belytschko, T. and Lu, Y.Y. (1994), "Element free Galerkin methods", *J. Numer. Meth. Eng.*, **37**(2), 229-256.
- Benz, W. and Asphaug, E. (1995), "Simulations of brittle solids using smoothed particle hydrodynamics", *Comput. Phys. Commun.*, **87**(1-2), 253-265.
- Haeri, H. (2015), "Simulating the crack propagation mechanism of pre-cracked concrete specimens under shear loading conditions", *Strength Mater.*, **47**(4), 618-632.
- Haeri, H., Khaloo, A. and Marji, M.F. (2014), "A coupled experimental and numerical simulation of rock slope joints behavior", *Arab. J. Geosci.*, **8**(9), 7297-7308.
- Haeri, H., Khaloo, A. and Marji, M.F. (2015), "Experimental and numerical analysis of Brazilian discs with multiple parallel cracks", *Arab. J. Geosci.*, **8**(8), 5897-5908.
- Haeri, H., Shahriar, K., Marji, M.F. and Moarefvand, P. (2013), "Experimental and numerical study of crack propagation and coalescence in pre-cracked rock-like disks", *J. Rock Mech. Min. Sci.*, **67**, 20-28.
- Haeri, H., Shahriar, K., Marji, M.F. and Moarefvand, P. (2014), "On the cracks coalescence mechanism and cracks propagation paths in rock-like specimens containing pre-existing random cracks under compression", *J. Central South Univ.*, **21**(6), 2404-2414.
- Haeri, H., Shahriar, K., Marji, M.F. and Moarefvand, P. (2013), "A coupled numerical-experimental study of the breakage process of brittle substances", *Arab. J. Geosci.*, **8**(2), 809-825.
- Jiao, Y.Y., Zhang, H.Q., Tang, H.M., Zhang, X.L., Adoko, A.C. and Tian, H.N. (2014), "Simulating the process of reservoir-impoundment-induced landslide using the extended DDA method", *Eng. Geol.*, **182**, 37-48.
- Jiao, Y.Y., Zhang, H.Q., Zhang, X.L., Li, H.B. and Jiang, Q.H. (2015), "A two-dimensional coupled hydromechanical discontinuum model for simulating rock hydraulic fracturing", *J. Numer. Meth. Eng.*, **39**(5), 457-481.
- Jiao, Y.Y., Zhang, X.L. and Li, T.C. (2010), *Discontinuous Deformation Analysis for Modeling Jointed Rock Failure Process*, Science Press, Beijing, China.
- Lee, H.W. and Jeon, S.W. (2011), "An experimental and numerical study of fracture coalescence in pre-cracked specimens under uniaxial compression", *J. Solid. Struct.*, **48**(6), 979-999.
- Libersky, L.D., Petschek, A.G., Carney, T.C., Hipp, J.R. and Allahdadi, F.A. (1993), "High strain Lagrangian hydrodynamics: A three-dimensional SPH code for dynamic material response", *J. Comput. Phys.*, **109**(1), 67-75.
- Liu, R.C., Jiang, Y.J. and Li, B. (2016), "Effects of intersection and dead-end of fractures on nonlinear flow and particle transport in rock fracture networks", *Geosci. J.*, **20**(3), 415-426.
- Mahmoud, B., Kamran, G., Mohammad, F.M. and Aliakbar, G. (2014), "Numerical simulation of crack propagation in layered formations", *Arab. J. Geosci.*, **7**(7), 2729-2737.
- Mohammadi, M. and Tavakoli, H. (2015), "Comparing the generalized Hoek-Brown and Mohr-Coulomb failure criteria for stress analysis on the rocks failure plane", *Geomech. Eng.*, **9**(1), 115-124.
- Niroumand, H., Mehrizi, M.E.M. and Saaly, M. (2016), "Application of mesh-free smoothed particle hydrodynamics (SPH) for study of soil behavior", *Geomech. Eng.*, **11**(1), 1-39.
- Rabczuk, T. and Zi, G. (2007), "A meshfree method based on the local partition of unity for cohesive cracks", *Comput. Mech.*, **39**(6), 743-760.
- Scavia, C. (1999), *The Displacement Discontinuity Method for the Analysis of Rock Structures: A Fracture Mechanics*, in *Fracture of Rock*, WIT/Computational Mechanics, Boston, Massachusetts, U.S.A.
- Shi, G.H. (1988), "Discontinuous deformation analysis-a new numerical model for the statics and dynamics of block system", Ph.D. Dissertation, University of California, Berkeley, California, U.S.A.
- Shi, G.H. (1999), "Applications of discontinuous deformation analysis and manifold method", *Proceedings of the 3rd International Conference on Analysis of Discontinuous Deformation*, Vail, Colorado, U.S.A., June.
- Vasarhelyi, B. and Bobet, A. (2000), "Modeling of crack initiation, propagation and coalescence in uniaxial compression", *Rock Mech. Rock Eng.*, **33**(2), 119-139.
- Vesga, L.F., Vallejo, L.E. and Lobo-Guerrero S. (2008), "DEM analysis of the crack propagation in brittle clays under uniaxial compression tests", *J. Numer. Meth. Eng.*, **32**(11), 1405-1415.
- Wang, P.T., Yang, T.H., Xu T., Cai, M.F. and Li, C.H. (2016), "Numerical analysis on scale effect of elasticity, strength and failure patterns of jointed rock masses", *Geosci. J.*, **20**(4), 539-549.
- Wang, W. (2014), "The discontinuous deformation analysis considering the block internal coupling effect and plastic anchoring effect", Ph.D. Dissertation, Shandong University, Ji'nan, China.
- Yang, S.Q., Yang, D.S., Jing, H.W., Li, Y.H. and Wang, S.Y. (2012), "An experimental study of the fracture coalescence behavior of brittle sandstone specimens containing three fissures", *Rock Mech. Rock Eng.*, **45**(4), 563-582.
- Yoon, J. (2007), "Application of experimental design and optimization to PFC model calibration in uniaxial compression simulation", *J. Rock Mech. Min. Sci.*, **44**(6), 871-889.
- Zhang, X.L. (2007), "Study on numerical methods for modeling

- failure process of semi-continuous jointed rock mass”, Ph.D. Dissertation, Chinese Academy of Sciences, Wuhan, China.
- Zhang, X.P. and Louis, N.Y.W. (2012), “Cracking processes in rock-like material containing a single flaw under uniaxial compression: A numerical study based on parallel bonded-particle model approach”, *Rock Mech. Rock Eng.*, **45**(5), 711-737.
- Zhou, X.P., Bi, J. and Qian, Q.H. (2015), “Numerical simulation of crack growth and coalescence in rock-like materials containing multiple pre-existing flaws”, *Rock Mech. Rock Eng.*, **48**(3), 1097-1114.
- Zhou, X.P., Cheng, H. and Feng, Y.F. (2014), “An experimental study of crack coalescence behavior in rock-like materials containing multiple flaws under uniaxial compression”, *Rock Mech. Rock Eng.*, **47**(6), 1961-1986.
- Zhu, W.S., Chen, Y.J., Li, S.C., Yin, F.Q., Yu, S. and Li, Y. (2014), “Rock failure and its jointed surrounding rocks: A multi-scale grid meshing method for DDARF”, *Tunn. Undergr. Sp. Tech.*, **43**, 370-376.